Characterization of SH-SY5Y Neurons Subject to 92kHz Ultrasound Stimulation

Caracterización de Neuronas SH-SY5Y Sujetas a Estimulación por Ultrasonido de 92 kHz

Priya S. Balasubramanian

SUMMARY: Cellular microstructural changes due to ultrasound exposure are critical to understand and characterize in order to further the establishment of ultrasonics in cell and tissue engineering and medicine. In this study, neurite length, nuclear morphology, and cellular toxicity are assessed at varying intensities of 92 kHz ultrasound provided by a piezoceramic disk element and incident upon SH-SY5Y neurons *in vitro*. Findings suggest that stimulation increases neurite length up to 2.73 fold tested at $\alpha = 0.05$ in an intensity dependent manner. Additionally, stimulation causes a statistically significant ($\alpha = 0.05$) decrease in nuclear area and less elongated nuclei, by 1.78 fold and 1.38 fold respectively, also in an intensity dependent manner. For maximum transducer surface intensities ranging from 0 to 39.11 W/cm^2, the toxicity of 92 kHz ultrasound is assessed and a nontoxic range is determined using Caspase-3 and Annexin V staining, in addition to Calcium imaging via Calcein-AM staining. Intensities of up to 1.6 W/cm^2 are found to be nontoxic for the cells under the parameters used in this study.

KEY WORDS: Ultrasound; Cell Biology; *in vitro*; Neural Stimulation; Neural Differentiation; Ultrasound Transducers.

INTRODUCTION

Ultrasound has been used to influence and characterize cells in many ways ranging from image formation, stimulation of ion channels, cellular differentiation and proliferation, and cellular ablation (Chapelon *et al.*, 1993; Fenster & Downey, 1996; Tyler, 2011; Zhou *et al.*, 2016; Bergmeister *et al.*, 2018; Balasubramanian Lal, 2018; Balasubramanian, 2021). The characterization of ultrasonic influence on cells for commonly used frequencies ranging from 20 kHz to hundreds of MHz is of high interest given the commonality of ultrasound interface and use with cells and tissue within these frequency ranges, as it is crucial to understand efficacious doses that do not induce cellular apoptosis and induce desirable cellular morphological changes (Fenster & Downey; Tyler). Previous studies have characterized the effects of common frequencies of ultrasound on cells, but the vast majority of these characterizations are in the arena of ion channel modulation, and there is much less focus on the potential to engineer the cell with ultrasound and the various mechanically derived effects of ultrasound exposure on the cell (Tyler; Fomenko *et al.*, 2018). Asides from ultrasonic neuromodulatory characterizations, the biological effects of ultrasound specific to human neural cells, while a highly

relevant field to assess given the relevance to secondary effects of ultrasonic neuromodulation, is equally highly under-investigated. As such, there is a growing need to understand the potential long term changes that ultrasound might impart on the structure and morphology of the cell body and chromatin.

A few pioneering studies have investigated different categories of biological effects of ultrasound on cells. As outlined in Table I, research has been conducted in the arena of neuromodulation, neurite formation, cellular regeneration, chromatin level changes, and toxicity under ultrasonic stimulation. Neurite growth and retraction are both observed in an intensity dependent manner (Hu *et al.*, 2013; Lee *et al.*, 2014; Ventre *et al.*, 2018). Chromatin is often found to be more condensed (both morphologically and through fluorescence intensity of stained cells) (Noriega *et al.*, 2012). Cellular regeneration, differentiation, and past a certain threshold apoptosis are found to be enhanced, for the conditions as outlined in Table I. Key studies outline potentially harmful doses starting at delivered intensities of 0.14 W/cm^2 (Feril Jr. & Kondo, 2004; Su *et al.*, 2019). Mechanisms of cellular modulation caused by ultrasonic

Electrical and Computer Engineering, Cornell University, Cornell University, 616 Thurston Ave., Ithaca, 14853, NY, United States.

stimulation are highly variable, plausibly frequency dependent, and intensity dependent. Various studies cite acoustic streaming, acoustic radiation force, direct pressure wavefront, and thermal effects as potential modulators of gene level changes (Draper *et al.*, 1995; Barnkob *et al.*, 2012).

In the following sections, a study of the influence of 92 kHz ultrasonic stimulus from a piezoceramic transducer on SH-SY5Y neural cells is presented. Results provide an analysis of the morphological and viability changes imparted by a commonly used frequency of ultrasonic stimulus (92 kHz) on an in vitro neural system. 92 kHz ultrasound has a wavelength in water of 1.6 cm, which scales to the size of a small region of tissue highly applicable for clinical use and tissue engineering. When focused to a cm scale spot size, this frequency of ultrasound could be very useful in engineering and regenerating neural tissue or other tissue types. This is one of the first presented analysis of cell viability and morphological change of a SH-SY5Y neural cell culture system under the influence of kHz ultrasonics and can serve as a baseline for many more studies to build upon. These results are of high importance in the field of biological and biomedical ultrasound.

MATERIAL AND METHOD

The following subsections detail the materials and methods utilized to obtain the results presented. Reagents used include SH-SY5Y neuroblastoma cells acquired from Sigma Aldrich (94030304, Sigma Aldrich, St. Louis, MO, United States), Calcein-AM acquired from Sigma Aldrich (56496, Sigma Aldrich, St. Louis, MO, United States), Apoptosis and Necrosis Assays acquired from Biotium (30017, Biotium, Fremont, CA, United States), and Phalloidin acquired from Biotium (00030, Biotium, Fremont, CA, United States). Media reagents (Eagle's Minimum Essential Medium (EMEM, Sigma Aldrich, St. Louis, MO, United States), Retinoic Acid (302-79-4, Sigma Aldrich, St. Louis, MO, United States), Fetal Bovine Serum (FBS, Sigma Aldrich, St.Louis, MO, United States), Pen/Strep (P0781, Sigma Aldrich, St. Louis, MO, United States), Glutamine (G8540, Sigma Aldrich, St. Louis, MO, United States)) were acquired from Sigma Aldrich. A 92 KHz resonance transducer is acquired from STEMINC, and has Silver electrodes coating the SM211 material used as the piezoceramic actuator material, actuated in radial mode, with a sinusoidal input of varying intensity at the resonance frequency of 92 kHz, specified and tested by the vendor STEM-INC (SMD22T25R211WL, STEMINC Steiner & Martins, Inc., Davenport, Florida, United States), and confirmed experimentally (Polytec UHF-120, Polytec, Inc., Waldbronn, Germany).

Transducer Interface with Cell Culture. The interface of the 92 KHz resonance piezoceramic with the neural cell culture is depicted in Figure 1. The transducer is placed within 20 microns of the surface containing cells and is immersed in cell culture media. The electrodes are insulated from the aqueous media as to prevent electrical stimulus in conjunction with the ultrasonic stimulus. The SH-SY5Y cells are grown in medium with the specifications stated in Shipley *et al.* (2016). The cells are seeded in the base medium for 48 hours at an initial density of 5000 cells/cm2. (Shipley *et al.* (2016))After 48 hours, 300 seconds (5 minutes) of continuous wave 92 kHz ultrasound is applied to the cells at the specified intensities. The cells that act as a control receive no ultrasound stimulation but are still interfaced with the transducer material for 300 seconds, with no actuation waveform provided, to provide the best settings for the control. In order to measure the biological effects of ultrasound that are not immediately caused by exposure, cells are then incubated in Retinoic Acid enhanced medium with partial serum deprivation following recommendations from Shipley *et al.* for 24 hours prior to staining and characterization.
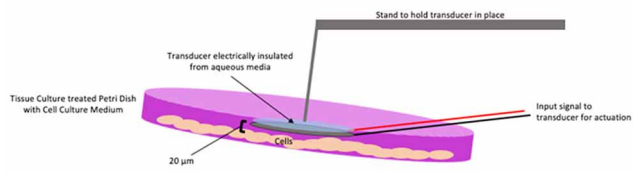

Fig. 1. Ultrasonic Transducer Interface with Cell Culture System. The experimental design layout, as described in the methods section, is visually depicted.

Neurite Quantification. In order to quantify the length of the neurites following ultrasound exposure, the cells are stained at the 24 hour time point post ultrasound exposure. Staining for neurite quantification is performed with fluorophore conjugated Phalloidin (ex/em 488 nm/517 nm, standard FITC) following standard fixation with formaldehyde. Imaging is performed on an upright microscope with broadband light source and FITC filtration under a 20x objective lens (Olympus BX51, Olympus Corporation, Shinjuku City, Tokyo, Japan). Exposure times are consistent and calibrated to image quality. Post processing of the image and quantification of neurite length is performed on ImageJ (ImageJ, National Institutes of Health, Bethesda, Maryland, United States). Neurites are traced when the extensions are < 5 μm in width. Contrast is matched and background is subtracted for display purposes. A total of 5 separate samples are analyzed with multiple cells in each sample.

Chromatin Characterization. In order to characterize the morphology of the nucleus and changes to the chromatin structure, cells are stained at the 24 hour time point with 4',6-diamidino-2-phenylindole (DAPI, ex/em 345/455 nm). Staining is performed following standard fixation with formaldehyde. Imaging is performed on an upright microscope with broadband light source and DAPI specific filtration under a 20x objective lens (Olympus BX51, Olympus Corporation, Shinjuku City, Tokyo, Japan). Exposure times are consistent and calibrated to image quality. Aspect ratio and area of the nucleus is evaluated through quantification on ImageJ (ImageJ, National Institutes of Health, Bethesda, Maryland, United States). A total of 5 separate samples are analyzed with multiple cells in each sample.

Cellular Health Assays. In order to determine the potential toxicities of ultrasound, various cell health assays are performed. Staining for markers of apoptosis and necrosis (active Caspase-3 and Annexin V) is performed 120 minutes following ultrasound exposure. Calcein AM cell permeate is used to test long term cell viability 24 hours following ultrasound exposure. Staining follows standard protocols described by vendors. Imaging is performed with a standard upright microscope with broadband light source and dye-specific filtration (Olympus BX51, Olympus Corporation, Shinjuku City, Tokyo, Japan). Exposure times and imaging parameters are optimized for image quality and kept constant across samples. Analysis is performed using ImageJ (ImageJ, National Institutes of Health, Bethesda, Maryland, United States) and Matlab (MATLAB R2020a, MathWorks, Inc., Natick, MA, United States).

RESULTS

Various characterizations pertaining to cell morphology and viability are analyzed in this study, similar to the areas of interest outlined in Table I from previous work in the field. Each section will present quantitative findings from relevant perspectives.

Table I. Current Progress in Cellular Characterizations Under the Influence of Ultrasonic Stimulus. Major findings in the field of ultrasonic stimulation of cells is presented in a categorical manner. Representative papers are chosen to provide insights into the reach of each sub topic in the area of ultrasonic interfaces with cells and tissue.

Cellular Effect	Relevant Studies	Findings
Neural Cell Ion Channel Modulation	Tyler (2011); Fomenko *et al.* (2018); Black-More *et al.* (2019); Babakhanian *et al.* (2012)	Ultrasound is able to stimulate or repress ion channel activation in an intensity dependent and cell lineage dependent manner. Commonly reported frequencies range from 100s kHz to 100s MHz, with frequencies lower and higher also reported but less commonly. Localization down to the tens of microns is the commonly reported minimum.
Neurite Growth or Retraction	Hu *et al.* (2013) Ventre *et al.* (2018) Lee *et al.* (2014)	Low intensity ultrasound has been found largely to increase neurite length and elicit differentiation, however Hu *et al.* (2013) describes neurite retraction at high intensity and power, low frequency settings.
Cellular Regeneration	Bergmeister *et al.* (2018) Zhou *et al.* (2016).	Axonal regeneration and cellular proliferation have been observed under low intensity, nontoxic ultrasonic stimulus intensities.
Chromatin Level Effects	Noriega *et al.* (2012) Wang *et al.* (2019)	Chromatin condensation, circular morphology, and gene-level mediated chromatin proper are consistently reported as morphological markers, with specific mechanisms varying by cell lineage. Cellular differentiation, which influences and is influenced by chromatin structuring, is often connected to stretch receptor mediated mechanisms
Toxicities	Su *et al.* (2019); Feril & Kondo (2004).	Intensities at or above 0.69 W/cm^2 are likely to promote cellular apoptosis (>10% of cells) in Feril *et al.* (2004), although threshold is variable with frequency, cell lineage, and power. Some studies (Su *et al.*, 2019) find that intensities of 0.14 W/cm^2 can induce early apoptosis.

Neurite Outgrowth Following Ultrasound Exposure. Figure 2 shows representative images per intensity (including control), and a graphical quantification of neurite length. It can be seen that all three intensities of ultrasound result in statistically significant increases in neurite length compared to the control sample.

Furthermore, the control group (n, number of cells = 185) demonstrates a p value of <0.001 when testing for a statistically significant difference amongst the four groups compared to any of the three intensities of ultrasound tested. The 0.39 W/cm² group (n = 74) has longer neurites than all other groups, including the control, 1.6 W/cm² (n = 85), and 9.8 W/cm² (n = 55) at a statistical significance of $\alpha = 0.05$. Error bars show standard deviation for all plots in Figure 2.
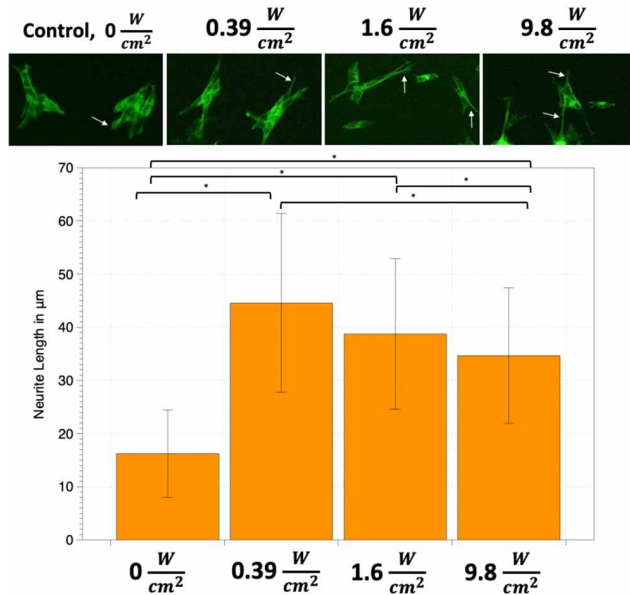

Fig. 2. Neurite Outgrowth Induced by Ultrasonics. Neurite outgrowth under different intensities of ultrasonic stimulation and control are depicted, with representative images shown and quantification provided. Error bars are standard deviation. Statistical analysis (ANOVA) and number of cells analyzed are presented in detail in the results section. Vertical dimension of image is 130μm. * represents significant difference at 0.05 significance level.

Chromatin Structural Changes Resulting from Ultrasonic Exposure. Figure 3 shows representative images per intensity (including control), and a graphical quantification of both nuclear aspect ratio and size as cross-sectional area. The nuclear cross-sectional area decreases with increasing stimulus intensity until the threshold of an intensity past 9.8 W/cm², when it again increases. The decrease in nuclear cross-sectional area is statistically significant for the control group (n, number of cells = 163),

0.39W/cm² (n=130) group, and 1.6 W/cm² (n = 170) group, which decrease significantly with increasing intensity. The 9.8 W/cm² group (n = 119) sees a statistically significant increase in nuclear cross-sectional area compared to the other two tested intensities and a comparable value to the control. The significance level of the comparison is at $\alpha = 0.05$. When performing an ANOVA analysis for the nuclear aspect ratio, the 0.39 W/cm² (n=130) group, and 1.6 W/cm² (n = 170) group are significantly smaller in aspect ratio compared to the control group (n = 163) and 9.8 W/cm² group (n = 119) at a significance level of $\alpha = 0.01$. Error bars show standard deviation for all plots in Figure 3.
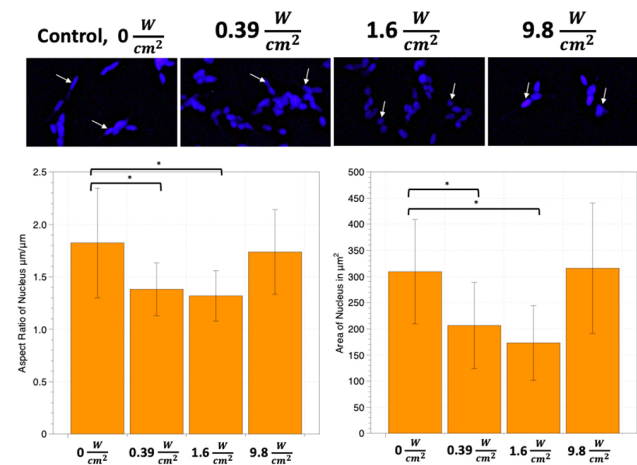

Fig. 3. Chromatin Condensation Induced by Ultrasonics. Chromatin structure under different intensities of ultrasonic stimulation and control are depicted, with representative images shown and quantification provided. Error bars are standard deviation. Statistical analysis (ANOVA) and number of cells analyzed are presented in detail in the results section. Vertical dimension of image is130μm. * represents significant difference at 0.05 significance level.

Cellular Viability Under kHz Ultrasonic Stimulus. Cellular viability is tested through Calcein-AM cell permeant loading. Results are shown in Figure 4 as a bar graph. Error bars are standard error. The control group (n, number of cells = 283), 0.39 W/cm² (n=352) group, 1.6 W/cm² (n = 233) group, and 9.8 W/cm² group (n = 121) are statistically higher in loaded intensity than the 39.1 W/cm² group. Cellular viability is further explored through Caspase-3 and Annexin V staining. The results of this analysis are more sensitive to ultrasound induced damage and related changes as they detect a lower threshold. These apoptosis and necrosis marker tests are performed in a smaller time span following ultrasound exposure (120 minutes). In this case, there is a significant increase compared to control in cellular apoptosis and necrosis markers for intensities ≥ 9.8 W/cm². Thus, the results of

this study support the conclusion that across these various different tests cell viability, maximum transducer surface intensities $\leq$ 1.6 W/cm^2 are safe for healthy cell culture utilizing SH-SY5Y neural cells as per protocols outlined in the methods section.
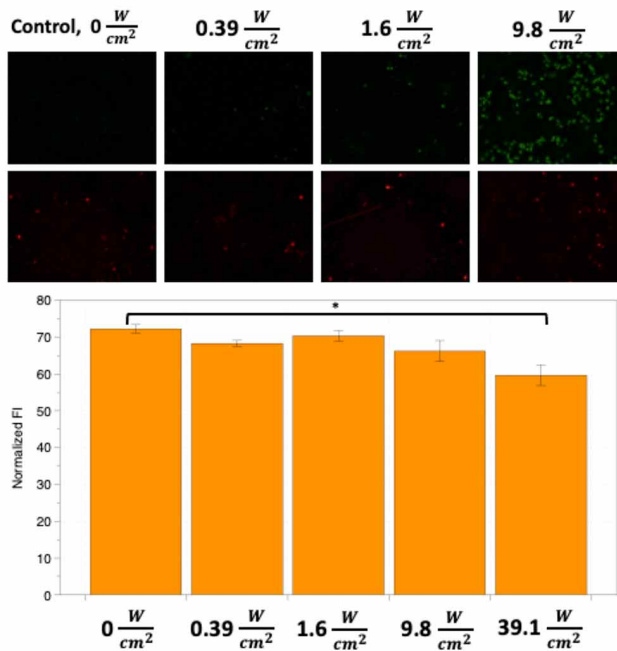

Fig. 4. Cellular Viability and Efficacious Dose of Ultrasonic Stimulus.Cellular viability under different intensities of ultrasonic stimulation and control are depicted, with representative images shown and quantification provided. Error bars are standard error. Statistical analysis (ANOVA) and number of cells analyzed are presented in detail in the results section. Vertical dimension of image is 665 μm. * represents significant difference at 0.05 significance level.

DISCUSSION

This study provides a broad range of effects of ultrasonic stimulus on human neural cells. The effects range from neurite outgrowth to chromatin structural changes, in addition to toxicity analysis of the kHz ultrasonic stimulus on neural cells. The claims of this study fit into the suggested behaviors of cells under ultrasonic stimulus in the body of supporting research as outlined in Table I. Neurite outgrowth and retraction have both been observed in previous studies. While these are seemingly contradictory results, it can be seen that the trend follows from a mechanical rationale that is intensity dependent. Studies with higher intensities of ultrasound observed neurite retraction, whilst low intensity (often low intensity and power through pulsed ultrasound delivery) ultrasound often results in neurite outgrowth (Hu

et al.; Ventre *et al.*). The results from this study, as outlined in Figure 2, show that, as expected, there is enhanced neurite growth at lower intensities when compared to control and then the neurite growth is stifled at higher intensities (evident in the data from the maximum surface intensity of 9.8 W/cm^2). Though for the highest intensity of 9.8 W/cm^2, the neurite length on average is still significantly larger than the control, it is also significantly smaller than the neurite lengths of the cells exposed to the lower intensities of ultrasound. The rationale for this closely follows a mechanics hypothesis. Lower intensities are more likely to stimulate differentiation through chromatin level effects, actin rearrangement of cytoskeletal matrix, and stretch receptor activation without being directly mechanically detrimental to the neurites through shear stress generation (Mobasheri *et al.*, 2002; Noriega *et al.*, 2013). The findings of study provide support to this claim with an intensity dependent result. The higher intensities past those displayed tend to result in very low cell densities due to the associated higher shear stresses. In future, it will be highly useful to probe the effect across a larger range of intensities with higher resolution in order to obtain a more accurate threshold to decouple competing factors. Furthermore, to isolate the effect of the direct pressure wave from streaming forces will be useful in determining mechanism. This could be accomplished by using a gel matrix substrate to grow cells in order to quell the fluid streaming or at least confine it to smaller sub-volumes that would not give highly directional movement and stresses on the cell body and neurites.

The chromatin level effects shown in Figure 3 follow findings in the literature as well (Noriega *et al.*, 2012). The highest intensity depicted, 9.8 W/cm^2, sees a reversal in the expected trend that is observed in the lower intensity stimuli. This is also coupled with low cell viability, as shown in Figure 4. Thus, it is probable that the nuclear morphology reverts because chromatin structural integrity is compromised or changed due to ultrasound induced damage. It can also be seen that the DAPI intensity is somewhat lower qualitatively for the 0.39 W/cm^2 and 1.6 W/cm^2 cases (Mascetti *et al.*, 2001; Noriega *et al.*, 2012). It can be observed with in vitro neural cell culture that elongation of neurites can to the elongation of the nucleus, through the Linker of Nucleoskeleton and Cytoskeleton (LINC) (Kim *et al.*, 2015; Balasubramanian *et al.*, 2020). However, in this case, coupling the results from Figures 2 and 3, it can be seen that the chromatin restructuring is not a result of neurite extensions. Ultrasound that enhances neurite outgrowth may also increase the aspect ratio of the nucleus due to the mechanical coupling between the nucleus and cytosol, but this is not the case in this study. As such, the chromatin restructuring is perhaps a direct result of mechanical stimulation by ultrasonics and strong enough to oppose the mechanical strain on the nucleus caused by neurite outgrowth.

The toxicity analysis and supporting conclusion presented in Figure 4 is supported by various literature. The maximal surface intensity of ≤ 1.6 W/cm^2 being nontoxic is similar to the findings of other relevant studies (Feril Jr. & Kondo). It should be noted that, as a limitation of this study and many other ultrasonic cell interface studies, the exact dosage of ultrasound incident upon the cell is highly variable and dependent on the transducer coupling with the medium (transmission losses), attenuation within the medium, and fluid coupling with cell culture medium that may cause acoustic streaming, in addition to thermal effects. As such, there is a strong need to expand the knowledge base in the area of ultrasound dose and mechanism, which will be critical to understanding the delivered dose that will be efficacious without being toxic to the cell.

Further future directions include gene level studies to understand the influence of ultrasonic stimulus on neural differentiation and proliferation. Additionally, a wider range and higher resolution of ultrasonic intensities will be tested. Decoupling fluid streaming from acoustic radiation force and the direct pressure wave will require spatial models of the interaction of the ultrasonic wavefront on cells in culture. Utilization of gel matrix scaffolds to culture cells can isolate effects further and minimize fluid streaming. Fluid motion quantification through microscopy and sensing techniques can allow for experimental validations of the effects of separate plausible mechanisms. This will ultimately be of high utility in uncovering underlying mechanisms and tuning efficacy towards engineering the cell and tissue of interest.

CONCLUSIONS

The results of this study define a threshold for kHz ultrasonic stimulus that retains cell viability whilst also influencing the morphology of the neural cell. Neurite elongation and nuclear level chromatin changes are pronounced under the influence of ultrasound. Future research will use this study as a baseline to investigate the mechanisms for such changes and toxicity thresholds in order to grow the field of ultrasonic stimulation towards tissue and cellular engineering.

BALASUBRAMANIAN, P. S. Caracterización de neuronas SH-SY5Y sujetas a estimulación por ultrasonido de 92 kHz. *Int. J. Morphol., 39(4)*:1109-1115, 2021.

RESUMEN: Los cambios micro estructurales celulares debidos a la exposición a los ultrasonidos son fundamentales para comprender y caracterizar el establecimiento de los ultrasonidos en la ingeniería y la medicina de células y tejidos. En este estudio, la longitud de las neuritas, la morfología nuclear y la toxicidad celular se evalúan a intensidades variables de ultrasonido de 92 kHz proporcionado por un elemento de disco piezocerámico e incidente sobre las neuronas SH-SY5Y *in vitro*. Los resultados sugieren que la estimulación aumenta la longitud de las neuritas hasta 2,73 veces probada a $\alpha = 0,05$ de una manera dependiente de la intensidad. Además, la estimulación provoca una disminución estadísticamente significativa ($\alpha = 0,05$) en el área nuclear y núcleos menos alargados, en 1,78 veces y 1,38 veces, respectivamente y también de una manera dependiente de la intensidad. Para intensidades máximas de la superficie del transductor que oscilan entre 0 y 39,11 W / cm^2, se evaluó la toxicidad del ultrasonido de 92 kHz y se determinó un rango no tóxico mediante tinción con Caspasa-3 y Anexina V, además de imágenes de calcio mediante tinción con Calceína-AM. Se encontró que las intensidades de hasta 1.6 W / cm^2 no son tóxicas para las células bajo los parámetros usados en este estudio.

PALABRAS CLAVE: Ultrasonido; Biología Celular; *in vitro*; Estimulación neural; Diferenciación neuronal; Transductores de ultrasonido.

REFERENCES

Balasubramanian, P. S. Nuclear elongation correlates with neurite induced cellular elongation during differentiation of SH-SY5Y neural cells. *Int. J. Morphol., 39(2)*:548-53, 2021.

Balasubramanian, P. S. & Lal, A. Cellular localization and dosage regulation of neural stimulation enabled by 1.05 GHz Ultrasonics. 2018 IEEE International Ultrasonics Symposium (IUS). IEEE, 1-4, 2018.

Balasubramanian, P. S.; Singh, A.; Xu, C. & Lal, A. GHz Ultrasonic chip-Scale Device induces ion channel Stimulation in human neural cells. *Sci. Rep., 10*:3075, 2020.

Barnkob, R.; Augustsson, P.; Laurell, T. & Bruus, H. Acoustic radiation- and streaming-induced microparticle velocities determined by microparticle image velocimetry in an ultrasound symmetry plane. *Phys. Rev. E Stat. Nonlin. Soft Matter Phys., 86(5 Pt. 2)*:056307, 2012.

Bergmeister, K. D.; Daeschler, S. C.; Rhodius, P.; Schoenle, P.; Böcker, A.; Kneser, U. & Harhaus, L. Promoting axonal regeneration following nerve surgery: a perspective on ultrasound treatment for nerve injuries. *Neural Regen. Res., 13(9)*:1530-3, 2018.

Chapelon, J. Y.; Faure, P.; Plantier, M.; Cathignol, D.; Souchon, R.; Gorry, F.; Gelet, A. The feasibility of tissue ablation using high intensity electronically focused ultrasound. *1993 Proceedings IEEE Ultrasonics Symposium, 2*:1211-4, 1993.

Draper, D. O.; Castel, J. C. & Castel, D. Rate of temperature increase in human muscle during 1 MHz and 3 MHz continuous ultrasound. *J. Orthop. Sports Phys. Ther., 22(4)*:142-50, 1995.

Fenster, A. & Downey, D. B. 3-D ultrasound imaging: a review. IEEE Eng. Med. Biol. Mag., 15(6):41-51, 1996.

Feril Jr., L. B. & Kondo, T. Biological effects of low intensity ultrasound: the mechanism involved, and its implications on therapy and on biosafety of ultrasound. *J. Radiat. Res., 45(4)*:479-89, 2004.

Fomenko, A.; Neudorfer, C.; Dallapiazza, R. F.; Kalia, S. K. & Lozano, A. M. Low-intensity ultrasound neuromodulation: An overview of mechanisms and emerging human applications. *Brain Stimul., 11(6)*:1209-17, 2018.

Hu, Y.; Zhong, W.; Wan, J. M. F. & Yu, A. C. H. Ultrasound can modulate neuronal development: impact on neurite growth and cell body morphology. *Ultrasound Med. Biol., 39(5)*:915-25, 2013.

Kim, D. I.; Birendra, K. C. & Roux, K. J. Making the LINC: SUN and KASH protein interactions. *Biol. Chem., 396(4)*:295-310, 2015.

Lee, I. C.; Lo, T. L.; Young, T. H.; Li, Y. C.; Chen, N. G.; Chen, C. H. & Chang, Y. C. Differentiation of neural stem/progenitor cells using low-intensity ultrasound. *Ultrasound Med. Biol., 40(9)*:2195-206, 2014.

Mascetti, G.; Carrara, S. & Vergani, L. Relationship between chromatin compactness and dye uptake for in situ chromatin stained with DAPI. *Cytometry, 44(2)*:113-9, 2001.

Mobasheri, A.; Carter, S. D.; Martín-Vasallo, P. & Shakibaei, M. Integrins and stretch activated ion channels; putative components of functional cell surface mechanoreceptors in articular chondrocytes. *Cell Biol. Int., 26(1)*:1-18, 2002.

Noriega, S.; Budhiraja, G. & Subramanian, A. Remodeling of chromatin under low intensity diffuse ultrasound. *Int. J. Biochem. Cell Biol., 44(8)*:1331-6, 2012.

Noriega, S.; Hasanova, G. & Subramanian, A. The effect of ultrasound stimulation on the cytoskeletal organization of chondrocytes seeded in three-dimensional matrices. *Cells Tissues Organs, 197(1)*:14-26, 2013.

Shipley, M. M.; Mangold, C. A. & Szpara, M. L. Differentiation of the SH-SY5Y human neuroblastoma cell line. *J. Vis. Exp., (108)*:e53193, 2016.

Su, Z.; Xu, T.; Wang, Y.; Guo, X.; Tu, J.; Zhang, D.; Kong, X.; Sheng, Y. & Sun, W. Low-intensity pulsed ultrasound promotes apoptosis and inhibits angiogenesis via p38 signaling-mediated endoplasmic reticulum stress in human endothelial cells. *Mol. Med. Rep., 19(6)*:4645-54, 2019.

Tyler, W. J. Noninvasive neuromodulation with ultrasound? A continuum mechanics hypothesis. *Neuroscientist, 17(1)*:25-36, 2011.

Ventre, D.; Puzan, M.; Ashbolt, E. & Koppes, A. Enhanced total neurite outgrowth and secondary branching in dorsal root ganglion neurons elicited by low intensity pulsed ultrasound. *J. Neural Eng., 15(4)*:046013, 2018.

Zhou, X.; Castro, N. J.; Zhu, W.; Cui, H.; Aliabouzar, M.; Sarkar, K. & Zhang, L. G. Improved human bone marrow mesenchymal stem cell osteogenesis in 3D bioprinted tissue scaffolds with low intensity pulsed ultrasound stimulation. *Sci. Rep., 6*:32876, 2016.

Corresponding autor:
Priya S Balasubramanian
Cornell University
616ThurstonAve
Ithaca
New York14853
UNITED STATES

E-mail: psb79@cornell.edu